

Material Based Splashing of Water Drops

Kshitiz Garg, Gurunandan Krishnan, and Shree K. Nayar

Department of Computer Science, Columbia University, New York, NY, USA
Email: {kshitiz, gkguru, nayar}@cs.columbia.edu

Abstract

The splashing of a water drop is a fascinating phenomenon that results from a variety of complex interactions between the drop and the material it impacts. In general, the distribution of droplets of a splash depends on the drop size and velocity; the surface roughness, rigidity, and wetness; and the angle of impact. Given the number of factors involved, it is difficult to develop an analytical model for the splash distribution. Instead, we take an empirical approach. We have measured the splashing behaviors of 22 different materials that are commonly found in the real world. These materials can be broadly classified as rough (e.g., wood and brick), smooth (e.g., marble and glass), flexible (e.g., silk and paper), and miscellaneous (e.g., water and moss). We have developed a stochastic model for splash distribution that builds upon empirical models previously developed in fluid dynamics and meteorology. Our model is simple and only requires 7 coefficients for generating splashes for head-on impact for a material. A more general model for generating splashes for arbitrary impact angles (due to surface inclination or wind) requires 54 coefficients. The models of different materials may be combined to generate physically plausible splashes for novel materials that have not been measured. Our model is applicable for rendering splashes due to rain as well as water drops falling from large heights such as windowsills, trees, and rooftops.

1. Introduction

Capturing the interaction of water drops with scene elements is important in achieving realism. This is particularly crucial when rendering rain, where lack of interaction of falling drops with scene elements makes the scene appear disconnected from the rain. Other common scenarios include drops falling from large heights such as windowsills, trees and rooftops. Over the last few years numerous algorithms have been developed to realistically simulate some of these interactions, such as the flow of water drops on surfaces [KKY93, KZYN96, WMT05] and the merging and deformation of water drops [FHP98, WMT05]. However, the splashing of water drops, which is a visually prominent effect, has not received much attention.

The splashing of a drop is a fascinating phenomenon that involves complex interactions between the fluid and the surface it impacts. As a result, the dynamics of a splash depends on many factors – the material properties of the surface (roughness, rigidity, etc.), the properties of the falling drop (size, velocity, etc.), and the angle of impact. Figure 1 I(a,b) shows 3D visualizations of measured splash distributions for rusted iron and plastic samples with 0° inclination (head-on impact). The differences in the number of splash droplets and their trajectories arising from the differing material properties are significant. Figure 1 I(c-d) shows measured splashes for the same samples inclined at 30° to the direction of the

falling drop. The inclination causes strong biases in the velocities and the orientations of splash droplets. These examples illustrate that when a splash is rendered, it is crucial to take into account the material properties and the inclination of the surface.

Although splashing of drops has been extensively studied in various fields (fluid mechanics, meteorology, agricultural engineering, and mechanical engineering) there are very few works that focus on the dynamic aspect of splashes[†]. Some numerical and analytical methods have begun to emerge in the above fields and in graphics. However, these methods cannot account for the materials properties and hence cannot be used to render material dependent splashes.

In the absence of a comprehensive framework for rendering drop splashes, several approximate methods have been implemented. For example, in the ATI demo [Tat06], a single high-speed video of a splashing milk drop was used to add splashes in a rain scene. Using a single splash event for dif-

[†] There has been significant work on the simulation of the dynamics of large bodies of fluids (see [Igl04] for a recent survey). These studies are primarily focused on the effects of external forces and boundary conditions on the dynamics of a body of fluid. In the case of water drop splashes, the dynamics (and hence the appearance) is mainly driven by the physical properties of the impacted material.

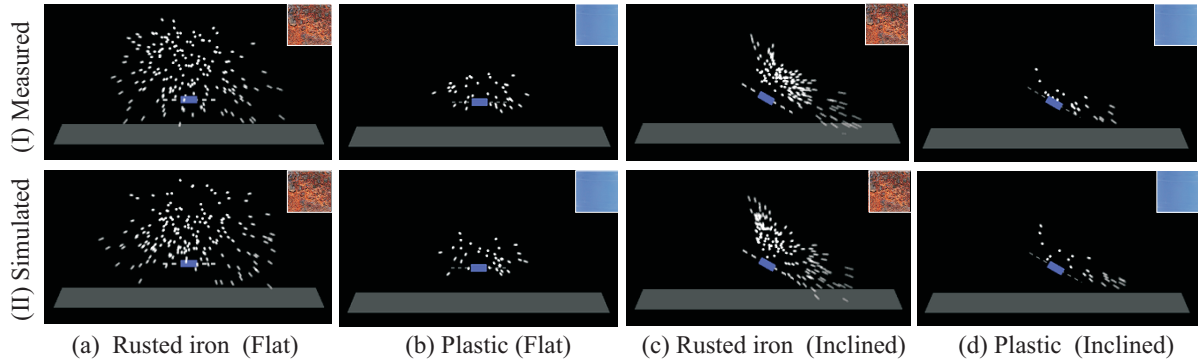


Figure 1: We have developed a compact data-driven stochastic model for realistic rendering of water drop splashes. Here we show 3D visualizations depicting splash trajectories as white motion-blurred streaks (I) 3D visualizations of measured splash distributions for (a) rusted iron at 0° (inclination), (b) plastic at 0° , (c) rusted iron at 30° , and (d) plastic at 30° . (II) The corresponding 3D visualizations of splash distributions simulated using the proposed model. The model is compact and yet accurately captures the effects of material properties and inclination on the splash distribution. Please see the video at [Web07]

ferent materials, however, makes the splashes appear repetitive and limits realism. Modeling software such as Maya and Houdini use particle systems [Ree83, Sim90] along with a deformable model for rendering crown-like structures that occur in a splash. These methods, however, rely on an artist to specify the splash parameters which are generally obtained by observing real splashes. This approach was used to render material dependent splashes in the movie “The Matrix Revolutions”. Although this approach can produce realistic results it is cumbersome for a scene that includes many materials with different inclinations. Thornton [Tho06] has recently developed a plug-in for Maya that allows artists to easily design splashes. However, it still requires an artist to set these parameters.

In this work, we study water drop splashes, with an aim to develop a compact model which can be directly used with particle systems to render material and inclination dependent splashes. Given the lack of understanding of the complex physical interactions involved during splash formation, it is difficult to develop a purely analytical model that accounts for material dependence. Therefore, we take a data-driven approach. The following are the main contributions of our work:

Measurement of Water Drop Splashes: We have developed a novel structured light method for measuring the 3D trajectories of the droplets produced by a splash. To capture the dependence on material and inclination we have measured 10 splash events per inclination angle, as the inclination is varied from 0° to 50° in steps of 10° . This set of splash measurements was obtained for 22 real-world materials that can be broadly classified as rough (e.g., brick and wood), smooth (e.g., marble and glass), flexible (e.g., silk and paper), and miscellaneous (e.g., water and moss). Figure 6 shows the complete list of materials that have been measured. In the case of 0° inclination (head-on impact), a thin liquid layer is formed on the surface that causes the formation of a crown-like structure immediately after impact. By taking side-view images of head-on splashes, we have measured the approx-

imate heights and radii of the crowns. These measurements are used with a generic crown model to render crowns for head-on impacts.

Stochastic Model for Rendering Water Drop Splashes:

Our measurements are used to develop a data-driven stochastic model that accurately captures the material and inclination dependencies of splashes. We use empirical probability models proposed in fluid dynamics and meteorology [SS77, MST95] to compute the means and standard deviations of splash droplet distributions. In particular, we use the Gaussian model for number distribution and velocity distribution. For the elevation angle distribution we use the three-parameter generalized extreme value model. These distribution models can be directly used with particle systems to render splashes. Our model is simple and only requires 7 coefficients for generating splashes for head-on impact for a material. A more general model for generating splashes for arbitrary impact angles (due to surface inclination or wind) requires 54 coefficients. Figure 1 II(a-d) shows 3D visualizations of splashes generated using our model, which can be seen to be in good agreement with the measured splashes in Figure 1 I(a-d). The model enables us to generate full 3D splashes and render them under arbitrary viewpoint and lighting. The splash coefficients of different materials can also be combined to generate physically plausible splashes for novel materials.

We conclude the paper by showing examples of rendered scenes with rain splashes. In each case, a single video of the scene was captured without rain. The recently proposed rain rendering algorithm of [GN06] was used to add rain to the video. Then, our splash model was used to add material-based splashes to the video.

2. Related Work

Splashing of liquid drops has intrigued researchers for more than a century. Worthington [Wor76, Wor08] appears to have been the first to qualitatively analyze the splashing nature of

drops by taking stroboscopic images of splashes. However, it was not until the 1950s that advances in several fields fueled a serious interest in splashing. Today, the physics of splashing is being explored in a variety of applications including printing (ink-jet printers), spraying (agriculture) and cooling of metals with liquid drops (manufacturing). Due to their importance, splashes have been studied in diverse fields such as fluid dynamics, meteorology, agricultural engineering, and mechanical engineering.

In most industrial applications, it is desirable that maximum spreading of drops is achieved without the formation of splashes. Most studies are therefore focused on the physical factors that avoid splash formation. An exception is the work by Stow and Stainer [SS77] which looks at the number, size, and distance distributions of splash droplets. They also study how the number of ejected droplets scale with the size and velocity of the falling drop. However, they do not consider the dynamic aspect of a splash, which is important in rendering.

Numerical methods [RF99, LGF04] have also been developed to simulate splashes on a thin film of liquid. These methods can be used to compute a full 3D splash at a high level of detail and at fine time scales. Unfortunately, these methods do not account for the roughness of the surface. Instead, they artificially introduce non-physical (e.g., Gaussian or sinusoidal) perturbations [RF99, BCM00, Yar06] to initiate splash formation. Hence, these methods cannot be used to render material-dependent effects. Furthermore, numerical simulations are computationally expensive and therefore are not suitable for rendering a large number of splashes, as is necessary in the case of rain. Analytical models for splashes are hard to develop given the complexity of the underlying physical processes. Recently, approximate theoretical models [YW95, RT02] have begun to emerge that explain the physical interactions that may be responsible for splash formations for thin liquid films. Rein [Rei93] and Yarin [Yar06] provide excellent reviews on the previous work on splashes.

As pointed out in [LH71, MST95, Yar06], there exists no comprehensive study on how splashing is influenced by the roughness of real-world materials or their inclinations. We believe our work takes a significant step in this direction. To our knowledge, our splash measurements represent the first dataset that capture the material and inclination dependent effects of splashing for real-world materials. In addition, we develop an empirical splash model that is effective in capturing the visual effects of material-based splashing. Recently, several image-based algorithms have been proposed for efficient rendering of rain [SW03, LZK*04, GN06]. These algorithms, however, do not address the rendering of splashes. We believe our work complements these algorithms.

3. Physics of Splashing

The complete physics of splash formation is rather complex and is beyond the scope of this paper. In this section, we describe the basics of splash formation and highlight the important physical factors involved.

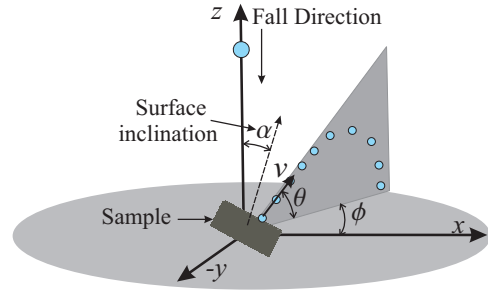


Figure 2: Parameters used to describe a splash event. The magnitude of the velocity of a droplet is denoted by v and its orientation is denoted by the elevation angle θ and the azimuthal angle ϕ . α is the inclination of the surface with respect to the fall direction of the drop (gravity).

3.1. Splash Formation

When a falling drop hits a surface, it is subjected to a sudden impact force. This impact deforms the drop and forces the water to flow radially outward. Some of the water eventually leaves the surface in the form of numerous small droplets – an event defined as a *splash*. Splashes can occur in two possible ways: (a) corona splash, where a thin crown-shaped water sheet rises vertically above the surface before breaking into smaller droplets, and (b) prompt splash, where droplets are emitted directly from the base of the drop without the formation of a crown. Typically, corona splashes occur in the presence of a thin liquid layer on surfaces with low inclinations. In almost all other cases, an impact results in a prompt splash (without a prominent crown).

3.2. The Parameters of a Splash

Splashing is inherently a random process, where each splash results in a unique set of droplets, each with different physical properties. A splash event can be characterized by the following parameters: **Number of droplets** (N); **droplet size** (radius a); **droplet velocity** (magnitude v); and **droplet orientation** (elevation angle θ , azimuthal angle ϕ). Additionally, in the case of a corona splash, the crown can be described by its height H and radius R . In our work, we do not model the sizes of droplets as these are hard to measure. Fortunately, differences in droplet sizes are hard to perceive from a drop splash. In applications where drop size is critical, the log-normal distribution can be used as suggested in [LH71, SS77].

3.3. Physical Factors Affecting a Splash

The physical factors influencing a splash can be divided into two main categories – drop-dependent factors and surface-dependent factors.

Drop Factors: The splashing of a water drop depends on its size and velocity[‡]. Empirical studies [SS77, SH81] have shown that an increase in the velocity of an impacting drop increases the number of resulting splash droplets as its square. Increase in the size (radius a_0) of the impacting drop, however, only increases the average size of the splash droplets. The effects of drop factors on crown parameters has also been studied. It has been shown that the radius R of the crown is proportional [Yar06] to $(2a_0)^{\frac{1}{4}} V_0^{\frac{1}{3}}$ and the height H is proportional [CMCZ04] to $(2a_0 V_0^2)^{\frac{2}{5}}$. These models can be used to generate splashes for water drops of different sizes and velocities.

Surface Factors: Real-world materials exhibit a wide variation in surface properties. Here, we briefly discuss the surface factors that strongly affect splashing.

Surface Roughness: Surface roughness is a critical factor that determines whether or not an impact will result in a splash. The disturbance in the drop caused by roughness at the time of impact is believed to be the main cause for splash formation [LH71, SS77, Yar06]. However, very little is known about the exact relation between surface roughness and the splash parameters.

Material Rigidity: Most previous studies have only considered drops falling on rigid surfaces. However, many real-world materials, such as paper and cloth, are not rigid. In general, non-rigid materials transfer less momentum and kinetic energy to the splash droplets, resulting in fewer droplets with lower velocities.

Surface Wetness: Empirical studies have shown that the wetness of a surface enhances its splashing behavior, producing larger numbers of droplets with larger sizes [SS77, MST95]. In this paper, we only consider splashes from steady-state wet surfaces, that is, surfaces that have been wet for some time.

Surface Inclination: Surface inclination makes the splash parameters strongly dependent on the azimuthal angle ϕ [Wri86] – more droplets (with lower elevation angles) emerge in the direction of inclination. The dependence on ϕ increases with the inclination angle. Studies [Wri86, SH81] have shown that splash dynamics is mainly determined by the velocity components of the drop parallel and perpendicular to the surface normal. Hence, splashing behavior for oblique impact depends mainly on the relative angle of impact.

Surface hydrophobia: Splashing is also affected by the hydrophobic nature of the surface – the physical aversion of a surface towards water. Hydrophobic surfaces often produce droplets with larger elevation angles [LH71]. Also, for large

[‡] Other drop factors such as surface tension and density also affect splashing but can be assumed to be constant in the case of water drops.

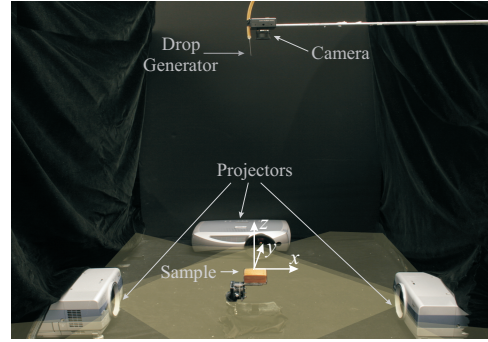


Figure 3: Apparatus used for measuring splash parameters. Three projectors are used to create a thin sheet of light below the sample material. Drops are produced using a drop generator and the sample is observed using a high-speed camera placed close to the generator. The splash droplets produce bright spots in the camera image when they pass through the sheet of light. The location and time at which each droplet passes the light sheet determines its velocity and orientation.

inclinations, they tend to produce droplets only in the direction of inclination.

While it is known that the above factors influence splashing, it is difficult to derive a comprehensive model from first principles that captures the effects of all the factors. For this reason, we take an empirical approach. We measure splashes from a variety of materials and develop a data-driven splash model that is built upon simple distribution functions that have been previously proposed.

4. Measurement of Splash Parameters

In this section, we describe a novel structured light method for measuring the parameters of a splash. Conventional approaches for shape measurement, such as stereo, are not suitable for splashes, as a splash produces a large number of visually identical droplets traveling at high velocities. Our structured light method exploits the fact that splash droplets travel along parabolic trajectories to efficiently and robustly estimate the orientation and velocity of each droplet.

4.1. Measurement Apparatus

Figure 3 shows the apparatus used for measuring splashes. Water drops of constant size (radius 1mm) are produced using a drop generator placed at a height of 5 m. This is done to ensure that drops reach a fixed velocity (near terminal velocity[§]) at the time of impact with the wet sample placed at ground level at the desired inclination angle. Drops falling on the sample result in splashes which are then imaged by a high-speed camera (PointGrey Dragonfly Express, operated

[§] Drops falling from a large height achieve a constant velocity after some time. This velocity is referred to as terminal velocity [GK49] and is given by $V_T = 200\sqrt{a_0}$, where a_0 is the drop's radius.

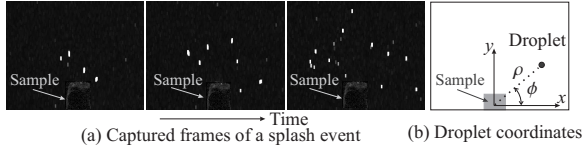


Figure 4: (a) Three frames (time instances) of a measured splash. The bright spots correspond to intersections of droplets with the light sheet. (b) ρ is the radial distance (in pixels) of the droplet from the center of impact and ϕ is its azimuthal angle measured from the x -axis.

at 60 fps) placed close to the drop generator. We use three projectors to create a thin, bright, horizontal sheet of light slightly below the sample[¶]. The splash droplets become visible as they pass through the light sheet. The time and location of the intersection of each droplet with the light sheet is detected from the captured video. Since the droplets must travel along parabolic trajectories, their intersections with the light sheet completely determine their trajectories. The end result is a complete space-time measurement of a splash – the evolution of a 3D droplet distribution over time.

Figure 4(a) shows three frames of the captured video of a splash from a mud sample. The bright white dots in the individual frames are the splash droplets as they pass through the light sheet. Figure 4(b) shows the coordinates of the intersection, as seen by the camera. The radial distance ρ of the droplet (in the image space) is proportional to the horizontal distance traversed before it intersects the light sheet. ϕ denotes the azimuthal angle measured from the x -axis.

4.2. Estimating Splash Parameters

We first find the locations of the light sheet intersections of splash droplets in each frame of the captured video. This is done by applying background subtraction and then sequential labeling. Each intersection yields the radial distance ρ and azimuthal angle ϕ of the droplet. These are used to compute its velocity magnitude v and elevation angle θ .

The horizontal distance D traversed by a droplet is simply given by $D = \frac{z_l}{f} \rho$, where f is the focal length of the camera (in pixels), ρ is the radial distance (in pixels), and z_l is the distance (in meters) of the light sheet from the camera. The time of flight of the droplet is given by $t = (n_f - n_i) / \omega$, where n_i is the frame in which the initial drop hits the surface, n_f is the frame in which the droplet intersects the light sheet, and ω is the frame-rate of the camera. The parabolic trajectory of a droplet can be written as:

$$D = v_x t, \quad h = -v_y t + \frac{1}{2} g t^2, \quad (1)$$

[¶] To maximize its brightness, the sheet is created only on one side ($y > 0$) of the sample (see Figure 4(b)). Since sample inclinations are made about the y -axis, the statistics of a splash are symmetric with respect to the x -axis, and hence it is sufficient to measure one half of the splash distribution.

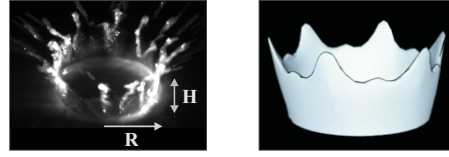


Figure 5: For low angles of inclination (head-on impact), some materials can produce corona splashes with crowns that appear for a short duration. The crown can produce noticeable effects when the splashes are viewed up close. The height and the radius of the crown vary between materials. We measure these parameters by taking a side-view image of the crown for each material, such as the one in (a). These measurements are used to scale the height and radius of the generic 3D crown model shown in (b) during rendering.

where, h is the vertical distance of the light sheet from the surface of the sample and $g = 9.8m/s^2$ is the acceleration due to gravity. From the above equations, we can solve for the horizontal velocity v_x and vertical velocity v_y . This gives us the velocity magnitude $v = \sqrt{v_x^2 + v_y^2}$ and the elevation angle $\theta = \tan^{-1}(v_y/v_x)$ of the droplet. Finally, the total number of droplets N equals the total number of bright dots (intersections) measured over all the frames. Thus, we have all the required parameters of the splash.

The finite resolution (640×480) and frame rate (60 fps) of the camera limits the accuracy of our measurements. However, this only introduces a small error – an error of ± 1 pixel is not visually perceptible, while an error of ± 1 frame lies within the sampling rate (30fps) of the human visual system. Considering that the average distance traversed by droplets before they intersect the light plane is 150 pixels and the average time is 18 frames these errors are insignificant and can be neglected.

One of the main advantages of using structured light is that the captured images contain only the information required for estimating the splash parameters. This allows for easy and accurate estimation of the parameters. On the other hand, if the entire splash region were to be illuminated, the captured images would reveal the entire trajectories of the droplets, making it harder to extract the relevant measurements.

Measuring Crown Parameters As mentioned earlier, drops impacting on surfaces with low inclination result in corona splashes which are characterized by the formation of crown-like structures. These structures can be visually prominent when viewed up close. In such settings, they need to be rendered in addition to the droplet distributions in order to achieve realism. To measure the crowns we use a high-speed camera (350 fps) to capture side-view images of splashes for each of our materials. These images show that crowns are mostly cylindrical in shape (also pointed out by Cosali [CCM97]). However, their heights and radii vary between materials. We roughly approximate the height and radius of



Figure 6: The 22 real-world materials for which we have made splash measurements. They have very different surface properties and can be broadly classified as rough, smooth, non-rigid, and miscellaneous.

the crowns (in their fully formed state) from the captured images. To render a crown we use a generic 3D model of a crown, shown in Figure 5. The height and radius of the generic model are scaled to account for the material dependency of the crown.

4.3. Splash Database with 22 Real-World Materials

We have used the above method to measure the splashing behaviors of 22 real-world materials. Figure 6 lists the different materials, which can be broadly classified into four categories – rough, smooth, non-rigid, and miscellaneous. The chosen materials sample a wide range of surface properties. For each material, we measured splashes at 6 different inclination angles that vary from 0° to 50° , in steps of 10° . We found that for inclination angles greater than 50° , the splashes are not visually prominent. Since splashes are inherently random, we have measured 10 splashes for each inclination of a material. In total, we have measured 1320 splash events.

5. A Stochastic Splash Model for Water Drops

Using the measured splash parameters, we develop a compact stochastic model for simulating new splashes. Our model builds upon empirical probability models previously proposed in fluid dynamics and meteorology. Our model computes the means and standard deviations of the splash distributions and hence can be directly used with particle systems for rendering splashes. We first discuss the model for head-on or low inclination impact and then a more general model which is valid for all surface inclinations for a material.

5.1. Splash Distribution Model for Head-on Impact

Since splashing is inherently random, splashes captured under identical conditions (same material and fixed inclination) will differ in terms of their measured parameters. Hence, we

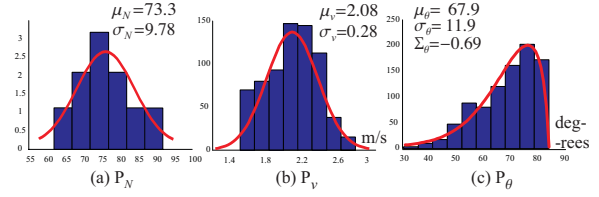


Figure 7: The splash number distribution P_N , velocity distribution P_V , and elevation angle distribution P_θ , for the wood sample for head-on impact. We use the Gaussian model for P_N and P_V and the generalized extreme value model for P_θ .

compute splash distributions from the 10 splashes measured for 0° inclination. Our data shows that the splash parameters - number(N), velocity(v), elevation angle(θ) and azimuthal angle(ϕ) are independent in this case. Our data also shows that the azimuthal angle follows a uniform distribution. Figure 7 shows the computed splash distributions for the wood sample.

To describe the distributions of the splash parameters, concisely, we use empirical probability models used in fluid dynamics and meteorology [SS77, MST95]. In particular, we use the Gaussian model $G(x; \mu, \sigma)$ for number distribution P_N and velocity distribution P_V . For the elevation angle distribution P_θ we use the three-parameter generalized extreme value model $F(x; \mu, \sigma, \Sigma)$ [KN01], where Σ is called the shape factor. Please see the Appendix for the exact form of generalized extreme value models. Figure 7 shows the results of fitting the above models (shown in red) to the measured splash distributions for the wood sample. As can be seen, the probability models fit the splash distributions quite well. This reduces the splash distributions to just 7 quantities, 2 each (mean and standard deviation) for describing the number and velocity distribution and 3 for describing the elevation angle distribution. These 7 coefficients can be directly used by particle systems to generate splashes for head-on impact.

5.2. Splash Distribution Model for Inclined Surfaces.

Surface inclination makes the splash distribution strongly dependent on the azimuthal angle ϕ and the inclination angle θ . To capture this dependence our model requires 54 coefficients. Figure 8 shows the basic steps used to derive the splash model for each material. We now discuss each of these steps in detail.

Computing Splash Distributions: As discussed in Section 3, the inclination α of the surface causes the splash parameters to be strongly correlated with the azimuthal angle ϕ . To capture this correlation, we model the splash parameter distributions as functions of (α, ϕ) . We discretize the measurements in the ϕ -dimension by dividing ϕ into small bins of size $\Delta\phi = 20^\circ$. The distribution of ϕ , $P_\phi(\alpha, \phi)$, is assumed to be uniform within each bin. We thus obtain the distributions of the splash parameters – number N , velocity v , and elevation angle θ – which are denoted by $P_N(\alpha, \phi)$, $P_V(\alpha, \phi)$, and $P_\theta(\alpha, \phi)$, respectively (see Figure 8(b)). There is no sig-

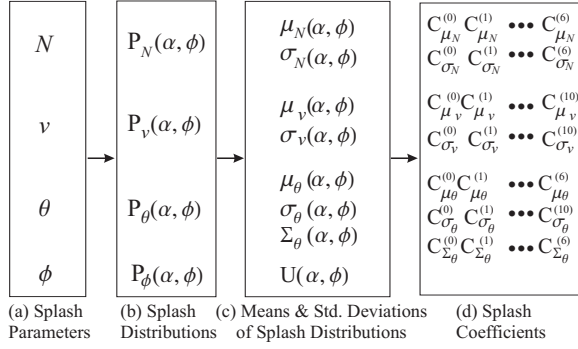


Figure 8: The pipeline used to estimate a compact splash model for each material. (a) The splash parameters (number, velocity, and orientation) measured using the structured light method. (b) A distribution is computed for each parameter, for each of the discrete values of (α, ϕ) . (c) We fit a probability model to each of these distributions to obtain its mean μ and standard deviation σ . (d) The means and standard deviations vary smoothly with α and ϕ . Low-order polynomial surfaces are used to compactly represent these variations. The final splash model of a material has a total of 54 coefficients.

nificant correlation between number, velocity and elevation angle distributions within the azimuthal angle bins. Figure 9 shows the splash distributions computed in this manner for the wood sample at an inclination of 30° . The top and bottom rows show the splash distributions for $\phi = 10^\circ$ and $\phi = 170^\circ$, respectively. Notice that the distributions vary significantly with ϕ .

Estimating Means and Standard Deviations of Splash Distributions: As in the case of flat impact, we use empirical probability models to describe the distributions. We use the Gaussian model $G(x; \mu, \sigma)$ for number distribution P_N and velocity distribution P_v , and the generalized extreme value model $F(x; \mu, \sigma, \Sigma)$ for elevation angle distribution. Figure 9 shows the results of fitting the above models (shown in red) to the measured splash distributions for the wood sample. As can be seen, the probability models fit the splash distributions quite well. Such fits are obtained for all the sets of discrete values of (α, ϕ) . As shown in Figure 8(c), this reduces the splash distributions to just 7 quantities, however, these are now functions of (α, ϕ) . The plots in Figures 10 and 11 show the estimated means and standard deviations of the fitted probability models as black dots for the wood sample. Notice that the means and standard deviations of each distribution vary smoothly with respect to α and ϕ .

The Final Splash Model For each splash parameter, we use a low-order polynomial surface to compactly represent the smooth variations of the mean and standard deviation with respect to α and ϕ . For the mean $\mu_N(\alpha, \phi)$ and standard deviation $\sigma_N(\alpha, \phi)$ of the droplet number distribution, we have used a 2nd order polynomial. As can be seen from Figures 10(a,b), good fits are obtained – the RMS errors are 5.13% and 6.25% respectively. Although smooth, the means

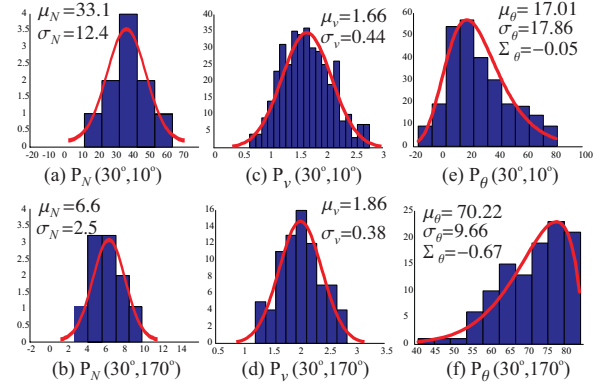


Figure 9: The splash distributions, $P_N(\alpha, \phi)$, $P_v(\alpha, \phi)$, and $P_\theta(\alpha, \phi)$, for the wood sample at an inclination of 30° . The top row shows the splash distributions for $\phi = 10^\circ$ (almost along the direction of inclination), while the bottom row shows the distributions for $\phi = 170^\circ$ (almost opposite to the direction of inclination). Notice the significant variations in the splash distributions with respect to ϕ . Based on previous studies, we use the Gaussian model for $P_N(\alpha, \phi)$ and $P_v(\alpha, \phi)$ and the generalized extreme value model for $P_\theta(\alpha, \phi)$.

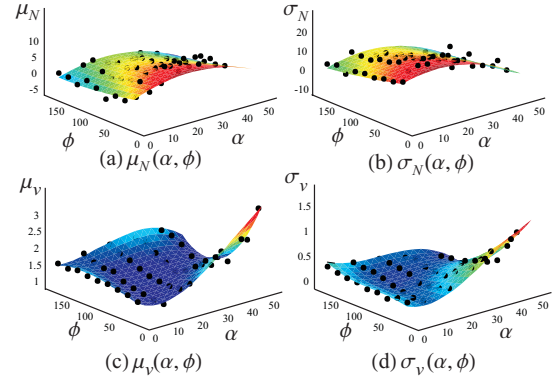


Figure 10: The black dots are the estimated means and standard deviations for (a,b) the number distributions and for (c,d) the velocity distributions for wood. While 2nd order polynomial surfaces fit the means $\mu_N(\alpha, \phi)$ and standard deviations $\sigma_N(\alpha, \phi)$ of the number distributions well, 3rd order polynomial surfaces are needed for the means $\mu_v(\alpha, \phi)$ and standard deviations $\sigma_v(\alpha, \phi)$ of the velocity distributions.

and standard deviations for the velocity distributions of most materials rise sharply for large inclination angles. To capture this effect, we have used 3rd order polynomial surfaces to represent $\mu_v(\alpha, \phi)$ and $\sigma_v(\alpha, \phi)$. As seen in Figures 10(c,d), good fits are obtained – the RMS errors are 5.63% and 4.16% respectively). Figure 11 shows similar surfaces obtained using polynomials of order 2 for the mean $\mu_\theta(\alpha, \phi)$, order 3 for the standard deviation $\sigma_\theta(\alpha, \phi)$, and order 2 for the shape factor $\Sigma_\theta(\alpha, \phi)$, of the elevation angle distribution. The RMS errors for these fits are 4.12%, 5.32% and 3.10% respectively.

The final splash model for each material consists of

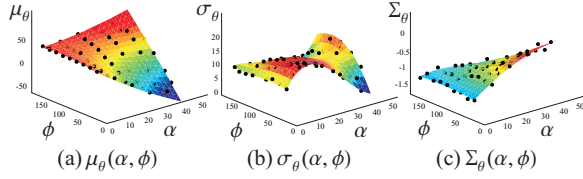


Figure 11: The black dots are the measured (a) means $\mu_\theta(\alpha, \phi)$ (b) standard deviations $\sigma_\theta(\alpha, \phi)$ and (c) shape factors $\Sigma_\theta(\alpha, \phi)$ of the elevation angle distributions for the wood sample. Fits of polynomial surfaces of order 2 were used for the means $\mu_\theta(\alpha, \phi)$ and shape factors $\Sigma_\theta(\alpha, \phi)$, while a surface of order 3 was used for the standard deviations $\sigma_\theta(\alpha, \phi)$.

a set of 7 surfaces which we denote by $M(\alpha, \phi) = [\mu'_N, \sigma'_N, \mu'_v, \sigma'_v, \mu'_\theta, \sigma'_\theta, \Sigma'_\theta]$. We use superscript (') to differentiate these functions from the computed ones shown in Figure 8(c). Each of these surfaces is completely specified by the coefficients of the polynomials. We refer to these coefficients as *splash coefficients* shown in Figure 8(d). A 3rd order polynomial surface requires 10 coefficients, while a 2nd order polynomial surface requires 6 coefficients. In total our model uses 54 coefficients to completely specify the splashing behavior of a material, including the effects of inclination. Figure 1 compares measured splashes with splashes simulated using our model for the rusted iron and plastic samples, for inclinations of 0° and 30° . Note that the simulated splashes appear very similar to the measured ones – the material and inclination effects are captured well. In Figure 12, we show the coefficients for 4 materials, one from each of our categories – rough, smooth, non-rigid, and miscellaneous. *Our database of estimated splash coefficients for all 22 materials is publicly available at [Web07].*

6. Rendering Water Drop Splashes

Rendering a splash consists of two steps – generating the splash parameters for droplets and rendering their appearances.

6.1. Generating Splash Parameters

Generating splashes for head-on impact is straightforward and is described in Section 5.1. Here we describe how a particle system generates splashes for arbitrary inclinations using our splash model. The user specifies the surface material and its inclination α . Once this information is provided, a splash is generated by following the pipeline shown in Figure 8, but in the reverse order, that is, from (d) to (a). We first use the material name to find the splash coefficients shown in Figure 8(d). These give us the set of seven surfaces $M(\alpha, \phi)$ that represent the means and standard deviations of the splash distributions. Next we discretize ϕ into bins^{||} of size $\Delta\phi$ and use M and α to compute the means and standard deviations of

^{||} This determines the coarseness of the sampling in ϕ . In our renderings, we set $\Delta\phi = 5^\circ$.



Figure 13: Splashes rendered using our method for a wood sample inclined at 35° . The dynamics of a splash is generated by following the steps shown in Figure 8 in the reverse order. All the droplets have the same appearance, which is rendered by ray-tracing (see inset image).

the splash distributions within each bin. These distributions are then sampled to get the final splash parameters for all the droplets (see Figure 8(a)). Since we are sampling probability distributions to generate splash parameters, each splash is unique, yet it accurately captures the material and inclination dependencies. Figure 1(II) shows splashes simulated using this method for rusted iron and plastic samples with inclinations of 0° and 30° .

Effect of Wind and Motion on Splashes: Our model can be easily used to render splashes affected by wind and surface motion. Due to wind, a falling drop will impact a flat surface at an oblique angle. As discussed in Section 3.3 the splash dynamics mainly depends on the relative angle of impact. Hence, the ejected droplet distribution for oblique impact is the same as the impact of a vertical drop falling on an inclined surface (apart from a rotation of the local coordinate frame). Therefore, our model can be used to obtain the initial droplet directions and velocities. The final trajectories of the individual droplets are determined by the direction of gravity and the wind forces. Also, splashes due to flat impact on moving surfaces are equivalent to splashes on an inclined surface [MST95].

Effect of Drop Size and Velocity on Splash: In this work we have measured the splashing behavior of water drops for fixed size and velocity. Studies in fluid dynamics (see Section 3.3) have modeled how the splash parameters are affected by drop size and velocity. These models can be used in conjunction with our model to generate splashes for water drops of different sizes and velocities.

6.2. Rendering a Splash

The appearance of a splash droplet at any time instant can be realistically rendered using ray-tracing. However, since a splash consists of a large number of transparent droplets, ray tracing the appearance of a splash at any time instant (with about 100 droplets) takes approximately 20 minutes on a Pentium4 3GHz computer. Clearly, ray-tracing even a few frames for rendering a motion blurred splash will take hours, making this approach impractical. Splashes can be very efficiently rendered by observing that each droplet is essentially a transparent sphere that acts like a lens with a large field of view of about 165° [GN03]. Since all the droplets in a scene see roughly the same environmental illumination, their appearances can be assumed to be more or less the same (ex-

Material		Number of droplets (N)	Velocity (v) (10^{-3} m/s ²)	Elevation angle (θ) (degrees)
Rough	 wood	$C_{\mu_N}=(17.02,0.38,-0.08,0.0,-0.01,0.0)$ $C_{\sigma_N}=(6.08,0.33,-0.04,0,-0.01,0.0)$	$C_{\mu_v}=(1715.7,44.2,2.95,-0.53,3.38,0.01,-0.01,0.0,-0.03,-0.0)$ $C_{\sigma_v}=(409.0,-21.44,3.00,-0.18,1.90,-0.04,0.0,0.0,-0.011,0.0)$	$C_{\mu_\theta}=(63.46,-3.04,0.12,0.02,0.01,0.0)$ $C_{\sigma_\theta}=(12.47,1.18,0.04,0.00,-0.06,0.0,0.0,0.0,0.0,0.0)$ $C_{\Sigma_\theta}=(-0.79,0.04,0.0,0.0,0.0,0.0)$
Smooth	 plastic	$C_{\mu_N}=(2.57,0.11,-0.03,0.0,-0.01,0.0)$ $C_{\sigma_N}=(1.73,0.15,-0.02,0.0,-0.00,0.0)$	$C_{\mu_v}=(1331.5,45.14,7.4,-0.67,4.2,0.08,-0.0,0.0,0.0,-0.0)$ $C_{\sigma_v}=(254.23,-2.16,1.07,0.22,0.40,-0.01,-0.0,-0.0,0.0,-0.0)$	$C_{\mu_\theta}=(0.05,-0.012,-0.01,0.0,0.0,0.0)$ $C_{\sigma_\theta}=(11.44,1.19,0.17,0.01,-0.07,-0.0,0.0,-0.0,0.0,0.0)$ $C_{\Sigma_\theta}=(32.56,-0.81,0.13,0.01,-0.01,-0.0)$
Non-rigid	 paper	$C_{\mu_N}=(11.78,0.3,-0.9,-0.01,-0.01,0.0)$ $C_{\sigma_N}=(6.51,0.05,-0.06,-0.0,-0.01,0.0)$	$C_{\mu_v}=(1519.41,-14.9,0.46,-0.32,1.94,0.01,-0.0,0.0,-0.0,-0.0)$ $C_{\sigma_v}=(342.5,-12.95,0.10,-0.16,1.5^*,0.0,-0.0,0.0,-0.01,-0.0)$	$C_{\mu_\theta}=(63.46,-3.04,0.12,0.02,0.01,0.0)$ $C_{\sigma_\theta}=(22.7,-0.58,-0.04,0.0,0.0,0.0,-0.0,0.0,0.0,0.0)$ $C_{\Sigma_\theta}=(-0.609,0.033,0.00,0.00,0.00,0.0)$
Misc.	 mud	$C_{\mu_N}=(7.53,-0.01,-0.09,-0.0,0.0,0.0)$ $C_{\sigma_N}=(4.30,0.04,-0.03,-0.0,0.0,0.0)$	$C_{\mu_v}=(1786.1,-6.42,-1.4,0.13,-0.49,0.0,0.0,0.0,0.0,0.0)$ $C_{\sigma_v}=(477.15,-6.02,-2.5,0.1,0.1,0.03,-0.00,0.0,0.0,-0.0)$	$C_{\mu_\theta}=(16.46,-3.04,0.12,0.02,0.01,0.0)$ $C_{\sigma_\theta}=(16.28,0.17,0.08,-0.00,0.01,-0.0,0.0,0.0,0.0,0.0)$ $C_{\Sigma_\theta}=(-0.65,0.01,-0.0,0.0,0.0,0.0)$

Figure 12: The coefficients of the splash models of four materials. The splash coefficients are specified as a row vector in the following order: $(1, \alpha, \phi, \alpha\phi, \alpha^2, \phi^2, \alpha^2\phi, \phi^2\alpha, \alpha^3, \phi^3)$. A total of 54 coefficients are used to represent the complete splashing behavior of a material, including the inclination effects. Due to limited space the splash coefficients have been rounded up to the second decimal digit. Our database of estimated splash coefficients for all 22 materials is publicly available at [Web07].

cept for overall brightness differences). This assumption is further justified by the fact that the droplets are very small and are severely motion-blurred. Hence, we ray-trace a single transparent sphere and use the resulting appearance for all droplets in the scene. We render at high frame rate and average frames over time to obtain motion-blurred splashes. This method reduces the rendering time of a complete splash to just a few seconds without noticeably compromising realism. The rendering speed can be further improved by using analytic and semi-analytic models for motion-blur. Figure 13 shows splashes rendered using this method for wood inclined at 35° . Figure 14 shows splashes rendered for brick, metal, and plastic. Notice that the splashes look realistic both in terms of their appearances and their dynamics. Please see videos at [Web07].

To render the crown, we use the measured height and radius for the given material. Typically, a crown lasts for 10-20ms and when rendered at higher frame rate, appears in several frames. To render the evolution of a crown we scale its height and radius linearly with time. The appearance of the crown is obtained by ray-tracing. The frames are then added to obtain the motion blurred crown. After motion-blur the crown appears in a single frame or at most two frames.

6.3. Editing Splashes

Since our splash model uses simple probability models, the splashing behavior of different materials can be combined to simulate splashing from novel materials. The simplicity of the model also enables a user to intuitively edit the behavior of a splash.

Splashes from Novel Materials: Our model can generate physically plausible splashes for novel materials that are not in the measured set. This can be done by linearly combining the sets of surfaces M_1 and M_2 that represent the means and standard deviations of the splash distributions of two different materials. That is, the means and standard deviations M_{new} of

the new material are given by

$$M_{new} = (1 - \beta)M_1 + \beta M_2, \quad (2)$$

where, β is the blending constant. M_{new} is then used to generate splash parameters as described in Section 6.1. The above described method can be used to create splashes from surfaces with varying material properties like smoothness, rigidity, and flexibility by combining two or more representative materials.

User-Designed Splashes: Since our splash model directly relates to physical properties, a user can intuitively edit the model to create interesting visual effects. For instance, by simply adding *global biases* to the means and standard deviations of a splash's distribution, a user can modify the dynamics of the splash in a global sense (identically for all ϕ s). Adding a global bias to $\mu_\theta(\alpha, \phi)$ will cause splash droplets to be ejected at larger elevation angles, giving the splash more of a bounce. Similarly, a user can add global biases to the means μ_N and μ_v to control the number of droplets and their velocities, and to the standard deviations to control the chaotic nature of the splash.

In some cases, the user may want to control the dependence of the splash parameters on ϕ . We refer to this as introducing an *azimuthal bias*. The dependence of the means and standard deviations $M(\alpha, \phi)$ on ϕ for a given value of α , can be expressed** in terms of the difference $M(\alpha, \phi) - M(\alpha, 90^\circ)$. Scaling this difference by a constant factor S biases a splash event with respect to ϕ . The modified splash distributions are now defined by $M_{mod}(\alpha, \phi)$:

$$M_{mod}(\alpha, \phi) = M(\alpha, 90^\circ) + S(M(\alpha, \phi) - M(\alpha, 90^\circ)). \quad (3)$$

** The gradient of an inclined surface varies with ϕ , such that it is maximum along the inclination direction ($\phi = 0^\circ$) and zero in the perpendicular direction ($\phi = 90^\circ$). Therefore, the effect of surface inclination on splash droplets is maximum when $\phi = 0$ and zero when $\phi = 90^\circ$. Hence, for a given α , the difference, $M(\alpha, \phi) - M(\alpha, 90^\circ)$, is a measure of the dependence of M on ϕ .



Figure 14: Splashes rendered using our method for brick, metal and plastic samples. Note the significant difference in the dynamics of the splashes. Brick produces a large number of droplets. On the other hand, splashes from metal have fewer droplets and appear to bounce off the surface. In contrast, plastic produces very few droplets with flat trajectories.

$S > 1$ exaggerates the dependence on ϕ , while $0 \leq S < 1$ suppress it. Please see the video [Web07] for examples of splashing from novel materials and splash editing.

7. Rendering Splashes in Rain Scenes

We now show the results of using our splash model for rendering splashes in rain scenes. The user provides an image (or video) of a wet scene, an approximate depth map of the surfaces in the scene, a segmentation of the scene into different materials, and the scene illumination. For rendering the rain itself, we use the algorithm and rain streak data given in [GN06]. Splashes are then generated using particle systems at the locations where the raindrops intersect the scene surfaces. Splashes are rendered at higher frame rate and then added to get the motion-blurred streaks, as explained in Section 6.2. Please see the results at [Web07].

Car Scene: Figure 15 I(a) shows an image of a wet car. The scene includes the metal body of the car, its glass windshield, a newspaper and a wool cap^{††}. Figure 15 I(b) shows frames of the scene rendered with rain and splashes. Figures 15 (c-f) show selected image regions (at original resolution) to highlight the differences in the splashes due to material and surface inclination. Note that the splashes from the metal hood (smooth) have far fewer droplets than the splashes produced by the newspaper (rough). The splashes also differ in their trajectories – droplets from the metal hood have larger elevation angles (θ), making the splashes appear bouncy. On the other hand, the wool cap produces droplets with very low velocities compared to the metal hood and the newspaper. Also, note the effects of the inclinations of the glass windshield (50°) and the newspaper (30°). In both cases, a larger number of droplets with higher velocities are seen along the inclination directions.

Backyard Scene: Figure 15 II(a) shows a backyard scene that includes a plastic chair, a leather basketball, a waterproof jacket^{‡‡}, bricks and concrete. Figure 15 II(b) shows frames of the scene with rendered rain and splashes. We show four

^{††} For the wool cap we used the splash model of silk.

^{‡‡} For the waterproof jacket we have used the splash model for umbrella cloth.

different scene regions in Figures 15 II(c-f) to highlight the material and inclination dependent effects. Notice that the plastic chair produces splashes with few droplets while the rough surfaces (concrete and brick) produce splashes with large numbers of droplets with high velocities. The jacket produces flatter splashes with fewer droplets.

These results demonstrate that capturing the effects of material properties and surface inclination on splashes is important for achieving realism. Even though the exact trajectories and the number of splash droplets may not be perceptible due to the fast nature of the phenomenon, the overall differences in terms of number of droplets, the horizontal and vertical extents and the shapes of the splashes are perceptible and are important for realism.

8. Conclusion

We have taken an empirical approach to modeling and rendering water drop splashes with material and inclination effects. Using a novel structured light method, we have measured 3D splash distributions for a total of 22 different real-world materials. We believe that our splash measurements represent the first dataset for the material and inclination effects of splashing. We have used these measurements to develop a compact stochastic model for realistic rendering of water drop splashes. The model only requires 7 coefficients to generate splashes for head-on impact and 54 coefficients to specify the complete splashing behavior for any arbitrary inclination for a given material. It can also be used to generate physically plausible splashes from novel materials as well as to edit a splash's behavior by using intuitive controls. We believe that our measurements and our splash model provide a convenient way to render splashes due to rain as well as water drops falling from large heights such as windowsills, trees, and rooftops. We believe that this work will be very helpful to artists and in the production industry.

Since splashing depends on a large number of factors it is difficult to measure the effects of all of them. We have measured and modeled the effects of material and surface inclination and have incorporated previous models to describe the effects of other factors such as size and velocity of the impacting drop, motion of the surface, and wind. The effects of surface wetness on splashes has not been modeled, as it is

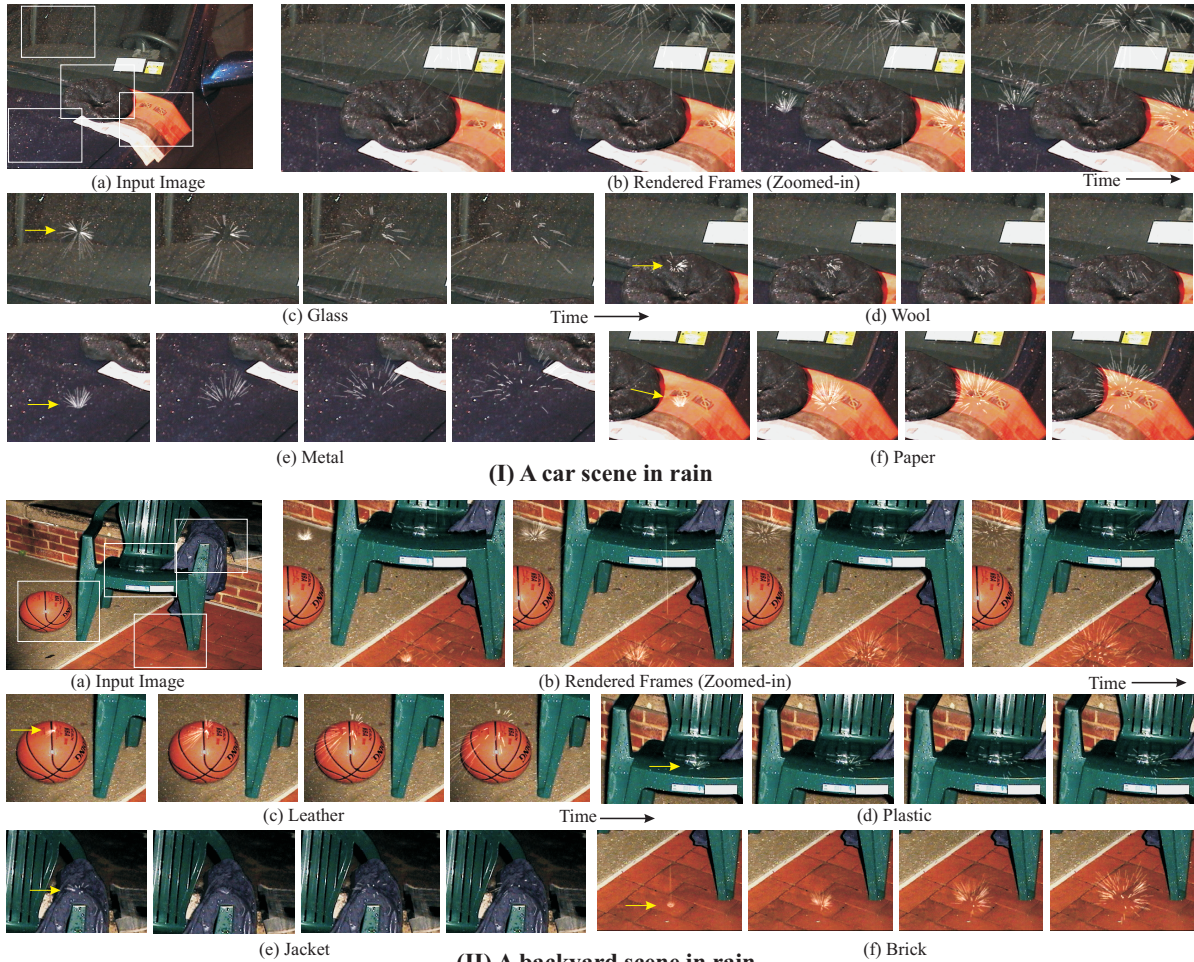


Figure 15: Rendering raindrop splashes in scenes. (I) Splashes rendered in a car scene. I(a) The input scene consists of a metal hood, a glass windshield, a newspaper, and a wool cap. I(b) Frames from the video rendered with rain and splashes. I(c-f) Selected image regions (white boxes in I(a)) at original resolution that highlight the differences in the splashes (see yellow arrows) due to material and inclination. Notice that paper produces a larger number of droplets than the smooth metal surface. Also, note the effects of inclination on the splash trajectories for glass and newspaper. (II) Splashes rendered in a backyard scene. II(a) The input image of the scene consisting of a plastic chair, a leather basketball, a waterproof jacket, and rough surfaces – brick and concrete. II(b) Frames from the video rendered with rain and splashes. II(c-f) Selected image regions (white boxes in II(a)). Note that the rough surfaces produce more droplets with higher velocities compared to plastic. Splashing is difficult to show using images. We request the readers to please see the videos at [Web07].

hard to control. In the future, we would like to study this effect. In this work, we have approximated the crown structure in corona splashes using a generic crown model. Devising techniques to measure the actual 3D crown structures is another challenging problem. Finally, we would like to implement our splash rendering algorithm using graphics hardware to achieve real-time performance.

Acknowledgement

This research was conducted at the Computer Vision Laboratory at Columbia University. It was supported in part by a grant from the Office of Naval Research (No. N00014-05-1-

0188) and a grant from the National Science Foundation (No. IIS-04-12759).

References

- [BCM00] BUSSMANN M., CHANDRA S., MOSTAGHIMIA J.: Modeling the splash of a droplet impacting a solid surface. *Physics of Fluids* 12 (2000), 3121–3132.
- [CCM97] COSSALI G., COGHE A., MARENGO M.: The impact of a single drop on a wetted solid surface. *Experiments in Fluids* 22 (1997), 463–472.
- [CMCZ04] COSSALI G., MARENGO M., COGHE A., ZH-

- DANOV S.: The role of time in single drop splash on thin film. *Experiments in Fluids* 36 (2004), 888–900.
- [FHP98] FOURNIER P., HABIBI A., POULIN P.: Simulating the flow of liquid droplets. In *Graphics Interface* (1998), 133–142.
- [GK49] GUNN R., KINZER G. D.: Terminal Velocity for Water Droplet in Stagnant Air. *Journal of Meteorology* 6 (1949), 243–248.
- [GN03] GARG K., NAYAR S.: Photometric Model for Raindrops. *Columbia Technical Report* (2003).
- [GN06] GARG K., NAYAR S. K.: Photorealistic Rendering of Rain Streaks. *ACM Trans. on Graphics (also Proc. of ACM SIGGRAPH)* (2006), 996–1002.
- [Igl04] IGLESIAS A.: Computer graphics for water modeling and rendering: a survey. *Future Generation Computer Systems* (2004).
- [KKY93] KANEDA K., KAGAWA T., YAMASHITA H.: Animation of Water Droplets on a Glass Plate. In *Proc. Computer Animation* (1993), 177–189.
- [KN01] KOTZ S., NADARAJAH S.: *Extreme Value Distributions: Theory and Applications*. World Scientific Publishing Company, 2001.
- [KZYN96] KANEDA K., ZUYAMA Y., YAMASHITA H., NISHITA T.: Animation of Water Droplet Flow on Curved Surfaces. In *Proc. Pacific Graphics* (1996), 50–65.
- [LGF04] LOSASSO F., GIBOU F., FEDKIW R.: Simulating water and smoke with an octree data structure. *ACM Trans. Graph.* 23, 3 (2004), 457–462.
- [LH71] LEVIN Z., HOBBS P.: Splashing of water drops on solid and wetter surfaces: Hydrodynamics and charge separation. *Phil. Transactions of the Royal Society of London Series* 269 (1971).
- [LZK*04] LANGER M., ZHANG L., KLEIN A. W., BHATTIA A., PEREIRA J., REKHI D.: A Spectral-particle Hybrid Method for Rendering falling Snow. In *Rendering Techniques* (2004), pp. 217–226.
- [MST95] MUNDO C., SOMMERFELD M., TROPEA C.: Droplet-wall collisions: Experimental studies of the deformation and breakup process. *Int. Journal Multiphase Flow* 21, 2 (1995), 151–173.
- [Ree83] REEVES W. T.: Particle System a Technique for Modeling a Class of Fuzzy Objects. *ACM Trans. Graphics* 2, 2 (1983), 91–108.
- [Rei93] REIN M.: Phenomena of liquid drop impact on solid and liquid surfaces. *Fluid Dynamics Research* 12 (1993), 61–93.
- [RF99] RIEBER M., FROHN A.: A numerical study of the mechanism of splashing. *Int. Journal Heat Fluid Flow* 20 (1999).
- [RT02] ROISMAN I., TROPEA C.: Impact of a drop onto a wetted wall: description of crown formation and propagation. *Journal of Fluid Mechanics* 472 (2002), 373–397.
- [SH81] STOW C., HADFIELD M.: An experimental investigation of fluid flow resulting from the impact of a water drop with an unyielding dry surface. *Proc. of Royal Society of London* 373 (1981).
- [Sim90] SIMS K.: Particle Animation and Rendering using Data Parallel Computations. *ACM SIGGRAPH '90* (1990), 405–413.
- [SS77] STOW C., STAINER R.: The Physical Products of a Splashing Water Drop. *Journal of Meteorological Society of Japan* 55, 5 (1977).
- [SW03] STARIK K., WERMAN M.: Simulation of Rain in Videos. *Texture Workshop, ICCV* (2003).
- [Tat06] TATARCHUK N.: Artist-directable real-time rain rendering in city environments. In *SIGGRAPH '06: ACM SIGGRAPH 2006 Courses* (2006), pp. 23–64.
- [Tho06] THORNTON J.: Directable Simulation of Stylized Water Splash Effects in 3D Space. *SIGGRAPH '06: ACM SIGGRAPH 2006 Sketches* (2006).
- [Web07] WEBSITE: <http://www.cs.columbia.edu/CAVE/>.
- [WMT05] WANG H., MUCHA P., TURK G.: Water Drops on Surfaces. *ACM Trans. on Graphics (also Proc. of ACM SIGGRAPH)* (2005).
- [Wor76] WORTHINGTON A.: On the forms assumed by drops falling vertically on a horizontal plate. *Proc. of Royal Society of London* 25 (1876).
- [Wor08] WORTHINGTON A.: *A Study of Splashes*. Longmans, Green and Company, London, 1908.
- [Wri86] WRIGHT A.: A Physically-Based Model of the Dispersion of Splash Droplets Ejected from a Water Drop Impact. *Earth Surf. Proc. Landforms* 11 (1986).
- [Yar06] YARIN A.: Drop Impact Dynamics: Splashing, Spreading, Receding, Bouncing. *Annual Review of Fluid Mechanics* 38 (2006).
- [YW95] YARIN A., WEISS D.: Impact of drops on solid surfaces: self-similar capillary waves, and splashing as a new type of kinematic discontinuity. *Journal Fluid Mechanics* 283 (1995).

Appendix

The generalized extreme value distribution is given by

$$F(x; \mu, \sigma, \Sigma) = \frac{1}{\sigma} (1 + \Sigma z)^{-1/\Sigma - 1} e^{-(1 + \Sigma z)^{-1/\Sigma}} \quad (4)$$

where, $z = \frac{x - \mu}{\sigma}$ and μ, σ, Σ represent the three parameters of the distribution – mean, standard deviation, and the shape factor respectively.